AMERICAN SOCIETY FOR MICROBIOLOGY | mBio®

RESEARCH ARTICLE

Inhibitory Concentrations of Ciprofloxacin Induce an Adaptive Response Promoting the Intracellular Survival of *Salmonella enterica* Serovar Typhimurium

Sushmita Sridhar,[a,b]* Sally Forrest,[a] Derek Pickard,[a] Claire Cormie,[a] Emily A. Lees,[c] Nicholas R. Thomson,[b,d] Gordon Dougan,[a] Stephen Baker[a]

[a]Department of Medicine, University of Cambridge School of Clinical Medicine, Cambridge, United Kingdom
[b]Wellcome Sanger Institute, Hinxton, United Kingdom
[c]Department of Paediatrics, University of Oxford, Oxford, United Kingdom
[d]Department of Infectious and Tropical Diseases, London School of Hygiene and Tropical Medicine, London, United Kingdom

ABSTRACT Antimicrobial resistance (AMR) is a pressing global health crisis, which has been fueled by the sustained use of certain classes of antimicrobials, including fluoroquinolones. While the genetic mutations responsible for decreased fluoroquinolone (ciprofloxacin) susceptibility are known, the implications of ciprofloxacin exposure on bacterial growth, survival, and interactions with host cells are not well described. Aiming to understand the influence of inhibitory concentrations of ciprofloxacin *in vitro,* we subjected three clinical isolates of *Salmonella enterica* serovar Typhimurium to differing concentrations of ciprofloxacin, dependent on their MICs, and assessed the impact on bacterial growth, morphology, and transcription. We further investigated the differential morphology and transcription that occurred following ciprofloxacin exposure and measured the ability of ciprofloxacin-treated bacteria to invade and replicate in host cells. We found that ciprofloxacin-exposed *S.* Typhimurium is able to recover from inhibitory concentrations of ciprofloxacin and that the drug induces specific morphological and transcriptional signatures associated with the bacterial SOS response, DNA repair, and intracellular survival. In addition, ciprofloxacin-treated *S.* Typhimurium has increased capacity for intracellular replication in comparison to that of untreated organisms. These data suggest that *S.* Typhimurium undergoes an adaptive response under ciprofloxacin perturbation that promotes cellular survival, a consequence that may justify more measured use of ciprofloxacin for *Salmonella* infections. The combination of multiple experimental approaches provides new insights into the collateral effects that ciprofloxacin and other antimicrobials have on invasive bacterial pathogens.

IMPORTANCE Antimicrobial resistance is a critical concern in global health. In particular, there is rising resistance to fluoroquinolones, such as ciprofloxacin, a first-line antimicrobial for many Gram-negative pathogens. We investigated the adaptive response of clinical isolates of *Salmonella enterica* serovar Typhimurium to ciprofloxacin, finding that the bacteria adapt in short timespans to high concentrations of ciprofloxacin in a way that promotes intracellular survival during early infection. Importantly, by studying three clinically relevant isolates, we were able to show that individual isolates respond differently to ciprofloxacin and that for each isolate, there was a heterogeneous response under ciprofloxacin treatment. The heterogeneity that arises from ciprofloxacin exposure may drive survival and proliferation of *Salmonella* during treatment and lead to drug resistance.

KEYWORDS AMR, *Salmonella*, antimicrobial agents, cellular morphology, ciprofloxacin, confocal microscopy, transcriptomics

Citation Sridhar S, Forrest S, Pickard D, Cormie C, Lees EA, Thomson NR, Dougan G, Baker S. 2021. Inhibitory concentrations of ciprofloxacin induce an adaptive response promoting the intracellular survival of *Salmonella enterica* serovar Typhimurium. mBio 12:e01093-21. https://doi.org/10.1128/mBio.01093-21.

Editor Julian Parkhill, Department of Veterinary Medicine

Address correspondence to Stephen Baker, sgb47@medschl.cam.ac.uk.

* Present address: Sushmita Sridhar, Division of Infectious Diseases, Massachusetts General Hospital, Boston, Massachusetts, USA.

This article is a direct contribution from Gordon Dougan, a Fellow of the American Academy of Microbiology, who arranged for and secured reviews by David Rasko, University of Maryland School of Medicine, and Francesca Micoli, GSK Vaccines Institute for Global Health.

Received 5 May 2021
Accepted 19 May 2021
Published 22 June 2021

The current trajectory of resistance to numerous broad-spectrum antimicrobials in bacterial pathogens is steadily increasing, making antimicrobial resistance (AMR) of critical concern for human health. This problem is further exacerbated by the fact there are few novel antimicrobials in the developmental pipeline and a dearth of vaccines to prevent against the increasing number of drug-resistant bacterial infections (1, 2). A large burden of multidrug-resistant (MDR) organisms arise in low-to-middle-income countries (LMICs), which, in part, may be associated with high-level usage of broad-spectrum antimicrobials in the community (1). These factors pose a serious global health threat.

Fluoroquinolones are among the most commonly used broad-spectrum antimicrobials globally and are commonly administered for urinary tract infections, pneumonia, dysentery, and febrile diseases (3). This potent group of bactericidal chemicals act by binding to bacterial type II topoisomerases DNA gyrase I (GyrA and GyrB) and topoisomerase IV (ParC and ParE) to disrupt DNA supercoiling, which leads to cell death (4–6). Resistance to fluoroquinolones is associated with specific mutations in the *gyrA*, *gyrB*, *parC*, and/or *parE* genes, although the extent of resistance can be further modulated by mutations in efflux pumps and porins and also via the acquisition of plasmid-mediated quinolone resistance (PMQR) genes (7–11). Ciprofloxacin is the most widely available fluoroquinolone, and its common use, particularly in LMICs, has resulted in widespread resistance in once-susceptible pathogens (12–14).

Despite extensive resistance, ciprofloxacin remains commonly used, and given its mode of action, it is likely to induce a range of additional cellular responses (15). Transcriptional studies of bacteria exposed to ciprofloxacin have shown that pathways associated with the stress response, solute and drug transport, DNA repair, and phage induction are upregulated, which can increase error-prone DNA replication and bacterial resilience during ciprofloxacin exposure (16–21). However, little is known about how bacterial genotype influences the response to ciprofloxacin or how bacteria respond when exposed to inhibitory concentrations of the drug.

Salmonella enterica serovar Typhimurium is a Gram-negative enteric bacterium that typically causes a self-limiting gastroenteritis in humans but is also associated with invasive disease in the immunocompromised. Specific *S.* Typhimurium lineages, such as sequence type 313 (ST313) and ST34, are associated with invasive disease in parts of sub-Saharan Africa and Southeast Asia, respectively, and have independently developed resistance to ciprofloxacin multiple times (22, 23). AMR in these organisms typically arises during local outbreaks and is not ubiquitous, demonstrating that there can be variation in the AMR profile of individual bacteria belonging to a single clade.

Although the cellular mechanisms of ciprofloxacin resistance are well defined, our understanding of how bacteria evolve and adapt during short-term exposure to ciprofloxacin is limited. Specifically, there is a lack of evidence regarding how clinical isolates respond to antimicrobials they may commonly encounter indirectly during therapy. Here, aiming to understand how genotypic and phenotypic characteristics are impacted by fluoroquinolone exposure, we studied three diverse *S.* Typhimurium variants (ST313, ST34, and ST19) under sustained perturbation with ciprofloxacin. Focusing on an ST313 isolate, we found that bacteria have substantial resilience to high concentrations of ciprofloxacin and that ciprofloxacin-exposed bacteria undergo distinct morphological and transcriptional changes within a short time frame, impacting bacterial survival and their interactions with host cells.

RESULTS

***Salmonella* Typhimurium can replicate in inhibitory concentrations of ciprofloxacin.** Using three isolates of *S.* Typhimurium selected by sequence type (ST) and ciprofloxacin susceptibility, time-kill curves were performed in the presence of 0×, 1×, 2×, and 4× the ciprofloxacin MIC of each isolate to determine growth dynamics over a 24-h period of ciprofloxacin exposure (Fig. 1). Quantification of CFU demonstrated that bacterial growth was most likely to be inhibited between 0 and 6 h postexposure, and the rate of growth was dependent on ciprofloxacin concentration.

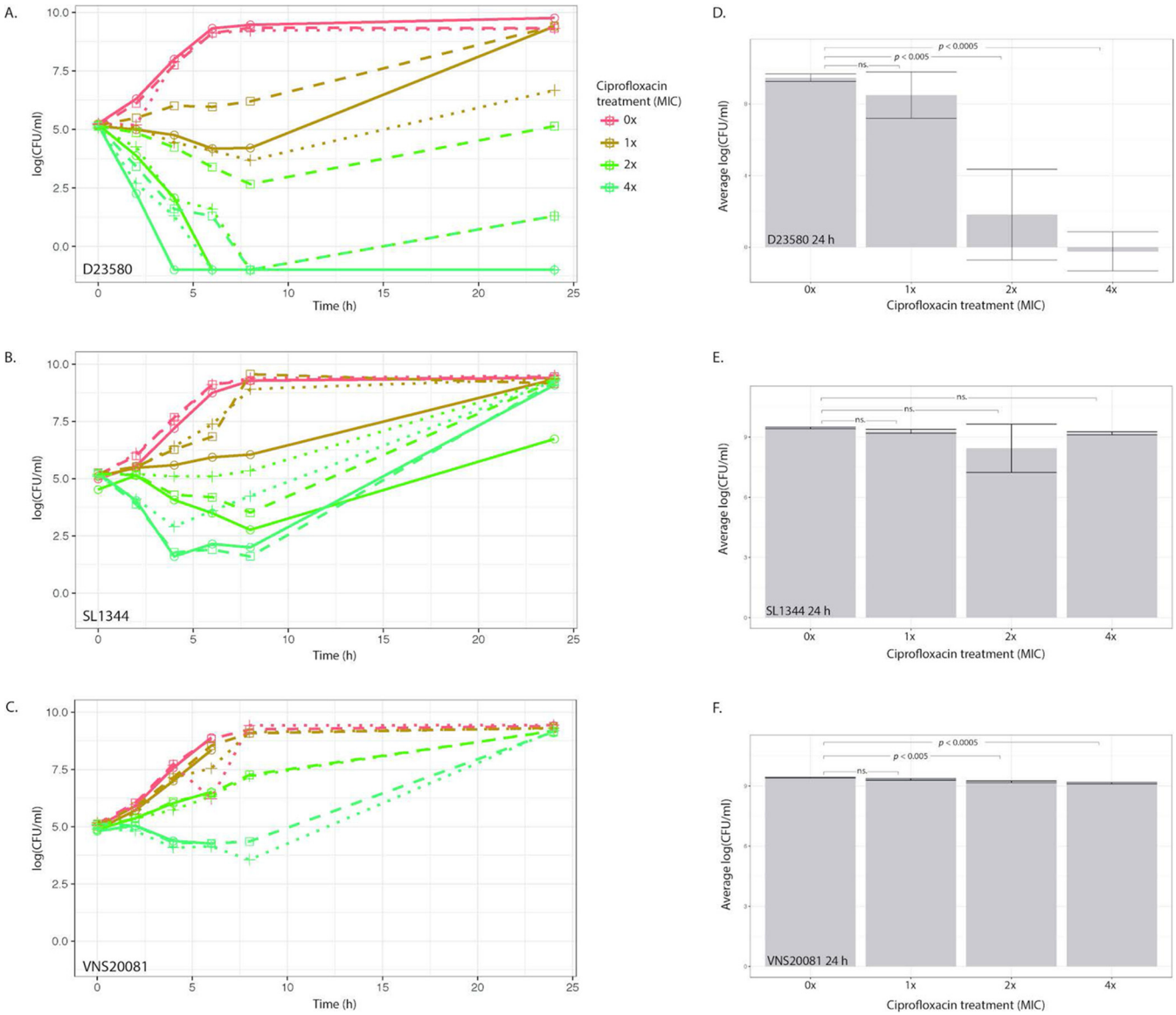

FIG 1 Time-kill curves of *S.* Typhimurium isolates at different ciprofloxacin concentrations. *S.* Typhimurium isolates D23580 (A), SL1344 (B), and VNS20081 (C) were grown for 24 h in four concentrations of ciprofloxacin (0×, 1×, 2×, or 4× MIC) and subjected to CFU enumeration at 6 time points post-inoculation. Three biological replicates were performed, and each replicate was plotted independently. The average CFU per milliliter was calculated for each isolate and condition for the 24-h time point and plotted as means ± SDs. (D) D23580; (E) SL1344; (F) VNS20081. An ANOVA was performed to compare means at 24 h, and Dunnett's test was performed to compare 24-h means of 1×, 2×, and 4× ciprofloxacin MIC to 0× (control).

However, after 6 h of ciprofloxacin exposure, there was a "recovery" phase, during which bacteria in the treated conditions began to replicate and increase in CFU (Fig. 1A to C). This trend was observed in all three isolates, although the degree of recovery and absolute number of organisms between isolates was variable. *S.* Typhimurium D23580 (ST313) bacteria showed the largest range of growth responses to different ciprofloxacin concentrations (Fig. 1A). All conditions of *S.* Typhimurium SL1344 (ST19) and *S.* Typhimurium VNS20081 (ST34) bacteria had comparable CFU values at 24 h, whereas there was considerably more variation in D23580 by treatment and replicate (Fig. 1D to F). In addition, after 8 h of exposure at 2× MIC of ciprofloxacin, the mean cellular concentration of D23580 was 153 ± 217 CFU/ml; under analogous conditions at 24 h, the mean CFU/ml was 46,000 ± 65,000 (Fig. 1A and D). The lower variability in SL1344 and VNS20081 cultures may be explained by their genetic backgrounds or specific ciprofloxacin MIC. Notwithstanding the experimental variation observed in D23580 cultures, the overall trend across multiple replicates of the three

isolates was that bacteria under high ciprofloxacin exposure were able to reach a concentration comparable to that of nontreated bacteria after 24 h.

We postulated that this recovery in growth was associated with ciprofloxacin degradation. To assess this, we centrifuged and filter sterilized the ciprofloxacin-containing medium after 24 h of bacterial growth. D23580 was inoculated into this filter-sterilized medium and incubated at 37°C for a further 24 h, as before. The time-kill curves replicated those of the original assays, indicating that the inhibitory activity of ciprofloxacin was preserved at approximately the same concentrations for the same time periods (see Fig. S1 in the supplemental material).

To determine whether the recovery of organisms under ciprofloxacin treatment was due to acquired mutations, we performed whole-genome sequencing on D23580 grown for 24 h without antimicrobial supplementation or with 0.06 μg/ml ciprofloxacin (2× MIC) to detect dominant single nucleotide polymorphisms (SNPs). To capture the genetic signatures of culturable organisms only, bacteria were grown in liquid broth for 24 h and then spread on agar plates. Colonies were pooled from each plate for DNA extraction and sequencing. Aiming to identify dominant mutations arising in D23580 across three biological replicates, we found mutations in *ramR* and *gyrA* in bacteria grown in ciprofloxacin. There were no mutations in untreated D23580. The occurrence of SNPs in *ramR* suggests that this gene plays a critical role in modulating bacterial survival during exposure to high ciprofloxacin concentrations in the absence of *gyrA* mutations (Table 1). Notably, only one of the three ciprofloxacin-treated cultures gained a *gyrA* mutation, which highlights the importance of studying other factors that may contribute to bacterial survival upon exposure to high doses of ciprofloxacin.

Ciprofloxacin induces morphological changes in *S.* Typhimurium. To better understand the impact of ciprofloxacin on the selected organisms, we exposed organisms D23580, SL1344, and VNS20081 to 0×, 1×, 2×, or 4× MIC of ciprofloxacin for 2 h and then imaged them using a quantitative high-content confocal microscopy system (24, 65). A time point of 2 h was selected to capture early adaptive responses. We found that the majority of ciprofloxacin-treated bacteria developed an elongated morphology within 2 h of ciprofloxacin exposure (Fig. 2). Some diversity in bacterial length upon ciprofloxacin treatment was apparent, suggesting a heterogeneous response to ciprofloxacin exposure. Quantitative image analysis of the lengths of individual organisms after 2 h indicated substantial heterogeneity in ciprofloxacin-exposed organisms and untreated bacteria (Fig. 2B to D). However, the mean length of nontreated bacteria was significantly less than that of ciprofloxacin-treated bacteria [D23580: 3.24 μm (0×), 6.73 μm (1×), 6.40 μm (2×), and 6.13 μm (4×), $P < 0.001$; SL1344: 2.89 μm (0×), 4.82 μm (1×), 6.73 μm (2×), and 6.70 μm (4×), $P < 0.001$; VNS20081: 3.24 μm (0×), 4.92 μm (1×), 6.54 μm (2×), and 7.23 μm (4×), $P < 0.001$]. Additionally, there also appeared to be variation in mean and maximum lengths of bacteria between the three isolates, with 4× MIC VNS20081 showing the greatest quantifiable change from untreated VNS20081 (mean of 7.23 μm versus 3.24 μm) (Fig. 2D). Moreover, there was not a uniform density distribution of cellular lengths; this observation was particularly apparent in the ciprofloxacin-treated bacteria. In particular, a number of 2× MIC ciprofloxacin-treated D23580 and VNS20081 bacteria elaborated considerable elongation, with lengths of >30 μm (Fig. 2B and D). Such a wide distribution of bacterial lengths indicates that ciprofloxacin exposure drives the formation of discrete bacterial populations of variable lengths.

Ciprofloxacin triggers isolate-specific transcriptional responses. Aiming to investigate the transcriptional features in the chromosome that may induce changes in survival and morphology, total RNA was extracted from the three isolates after 2 h of exposure to 2× MIC of ciprofloxacin and subjected to sequencing. This time point was selected to best capture early responses before significant cell death. Generally, the broad transcriptional profile was consistent between the three isolates; however, there was a significant difference in the number of genes significantly up- or downregulated under ciprofloxacin exposure compared to that with no treatment for D23580 ($-2 \geq \log_2$ fold change [$\log_2$fc] ≥ 2, $P < 0.05$) (D23580, 259 genes; SL1344, 165 genes;

TABLE 1 Dominant SNPs found after 24-h growth in 2× MIC ciprofloxacin

Replicate	SNP[a]	Gene containing SNP	Function
1	NA[b]	NA	NA
2	2981566	*ramR*	Regulator of AcrAB/TolC efflux pump
3	2399766	*gyrA*	DNA gyrase, DNA negative supercoiling

[a]SNP analysis to determine dominant SNPs was performed on *S.* Typhimurium D23580 grown for 24 h in 2× MIC ciprofloxacin compared against D23580 grown for 24 h without ciprofloxacin.
[b]NA, not available.

VNS20081, 160 genes) (Fig. 3; see also Data File S1 available at https://doi.org/10.17605/OSF.IO/N9CW5). Prophage and SOS response genes were among the most consistently highly upregulated regions in all isolates, and flagellar genes were most highly downregulated, although the number of genes and extent of upregulation were variable by isolate (Tables 2 and 3). Phage genes were not directly comparable between isolates, but in each isolate, they were the most highly upregulated genes, above SOS response genes (Fig. 3). The top upregulated SOS response genes in common between the three isolates were *recN*, *sulA*, *recA*, *uvrA*, *lexA*, *sodA*, and *polB*, all genes known to be integral to the early bacterial stress response to double-stranded DNA damage (25–27). Interestingly, there were also several metabolism- and biosynthesis-associated genes that were commonly upregulated (Table 2). Notably, other than flagellar genes, two downregulated genes in all isolates were *ompA* and *ompD*, which encode an outer membrane porin that plays a role in drug uptake and may be relevant in ciprofloxacin efflux (28–30). SL1344 had fewer downregulated genes with a $\log_2$ fold change of ≤ -2, and the genes were less clustered along the chromosome than those of D23580 and VNS20081 (Fig. 3B). Table S1 and Table S2 show the top 20 up- and downregulated genes for *S.* Typhimurium D23580, respectively. The majority of upregulated genes were in prophage regions; downregulated genes were overwhelmingly associated with flagellum and pilus formation (Fig. 3A). It is possible that D23580 had considerably more differentially expressed genes than SL1344 or VNS20081 because of a more robust prophage response.

Ciprofloxacin triggers a specific dose-dependent transcriptional response in D23580. To better understand the specificity of the bacterial stress response against ciprofloxacin, D23580 was subjected to four different perturbations, namely, 0.5× and 2× MIC ciprofloxacin, mitomycin C, and 1× MIC azithromycin, for 2 h prior to RNA sequencing. We chose D23580 to investigate further as it is an important clinical isolate for understanding invasive *Salmonella* disease and showed the most differential expression upon ciprofloxacin exposure. We found that each stressor induced a different transcriptional signature (Fig. 4; see also Data File S2 available at https://doi.org/10.17605/OSF.IO/N9CW5). We observed some overlap in transcriptional responses for the two concentrations of ciprofloxacin, suggesting that a subinhibitory ciprofloxacin concentration (0.5× MIC) elicits a reduced SOS response (with respect to that from 2× MIC), although upregulation of prophage genes was comparable. Furthermore, there were fewer downregulated genes in the subinhibitory concentration of ciprofloxacin than for 2× MIC (Fig. 4A and B). In contrast, treatment with mitomycin C, a potent inducer of double-stranded DNA breaks, elicited a notable prophage response (Fig. 4C) (31–34), but fewer SOS response genes were upregulated than under the ciprofloxacin-treated conditions, and overall fewer genes were differentially expressed. This was surprising, as we expected that mitomycin C would elicit a similar transcriptional signature to that for ciprofloxacin; however, these differences may have been due to the concentration of mitomycin C used. Such differences imply that while there is some overlap between the effects of ciprofloxacin and mitomycin C, they are not identical, and ciprofloxacin elicits a distinct stress response. Most notably, treatment with azithromycin, an azide antimicrobial that targets the 50S ribosomal subunit, elicited a unique transcriptional profile, with no overlapping genes with any of the other conditions, indicating that the mode of action of the antimicrobial induces a specific impact

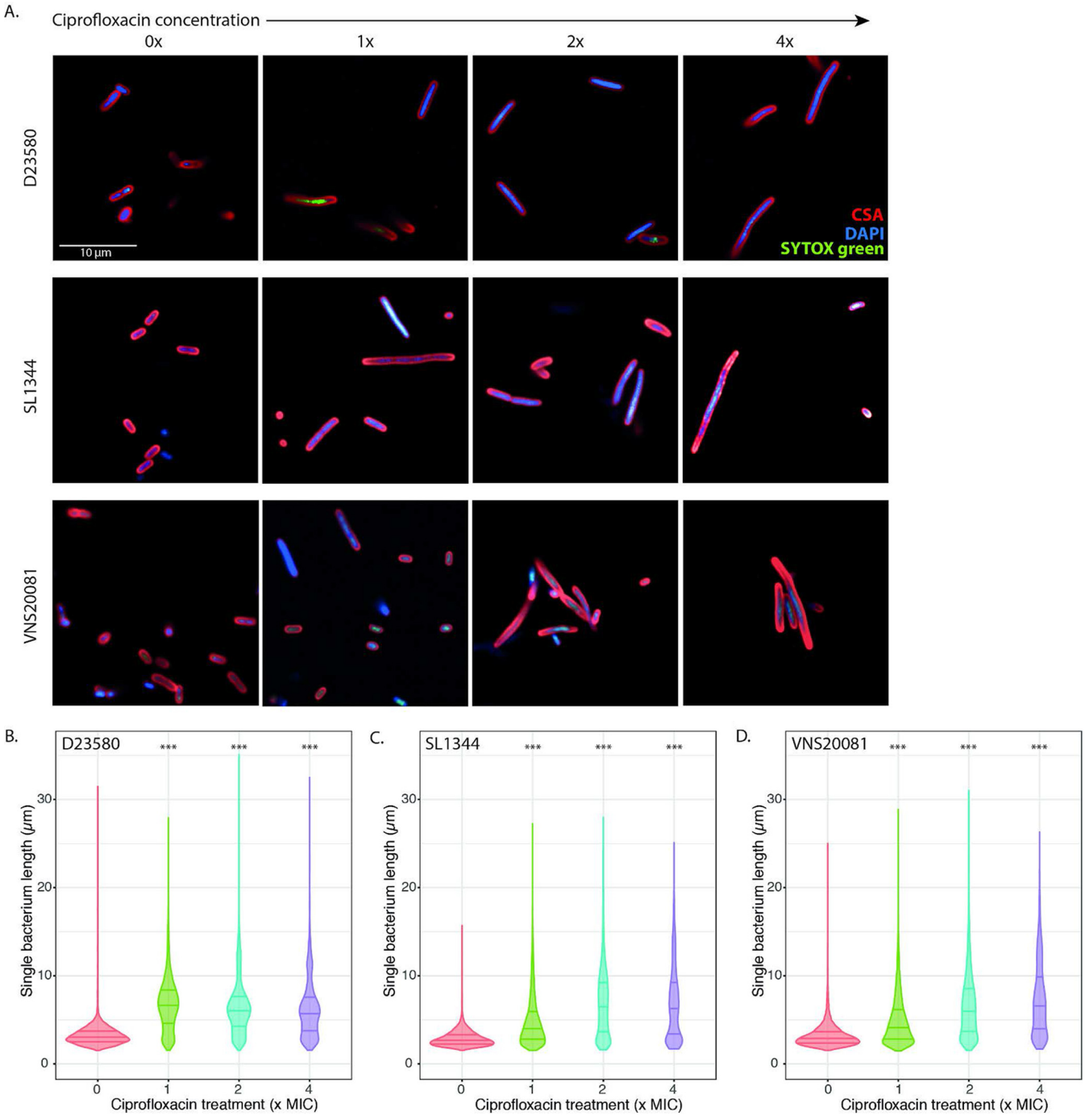

FIG 2 Imaging of *S.* Typhimurium following 2 h of ciprofloxacin exposure. (A) D23580 (top), SL1344 (middle), and VNS20081 (bottom) were subjected to 4 concentrations of ciprofloxacin (0×, 1×, 2×, or 4× MIC) and stained and imaged using an Opera Phenix high-content microscope. Bacterial membranes were stained using CSA (red), nucleic acids were stained using DAPI (blue), and permeabilized dead cells were stained using SYTOX green (green). Imaging experiments were carried out in triplicates, with two technical replicates; images from one replicate shown. (B to D) The length of single bacteria (μm) was measured quantitatively based on image analysis, and these were plotted for each isolate and condition independently (D23580, panel B; SL1344, panel C; VNS20081, panel D). Bacterial lengths were plotted as median and interquartile ranges, and the mean ± SD was calculated for each condition compared to 0× MIC treatment. One-way ANOVAs were performed. ***, $P < 0.0005$. 0×-treated bacteria are in red; 1×-treated bacteria are in green; 2×-treated bacteria are in blue; and 4×-treated bacteria are in purple.

on the transcriptional profile (Fig. 4D; see also Tables S3 and S4). Importantly, this signified that the transcriptional response to inhibitory concentrations of ciprofloxacin is distinct from that to azithromycin, and this difference may be useful for considering treatment options in clinical settings.

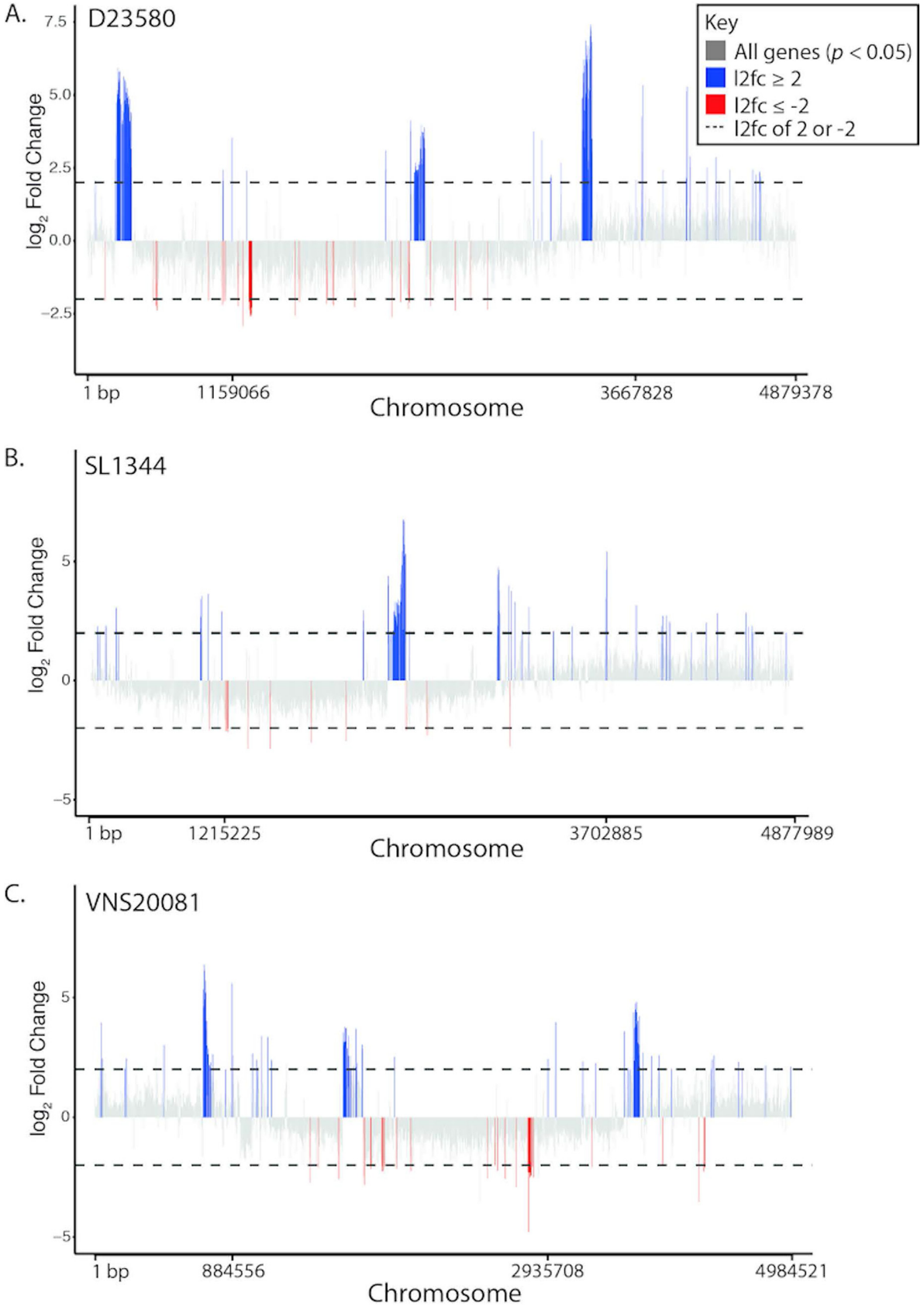

FIG 3 Bulk transcriptomics of *S.* Typhimurium following 2 h of ciprofloxacin treatment. *S.* Typhimurium isolates D23580 (A), SL1344 (B), and VNS20081 (C) were grown in medium containing either 0× or 2× MIC ciprofloxacin for 2 h, and RNA sequencing was performed.

(Continued on next page)

Ciprofloxacin exposure stimulates a heterogeneous population with distinct transcriptional profiles. As demonstrated above, ciprofloxacin exposure induced pronounced morphological changes across the bacterial population. We wanted to determine whether these morphologically distinct bacteria could be physically separated and classified as subpopulations based on different physical and transcriptional properties. To disaggregate the transcriptional profiles associated with the various populations formed during ciprofloxacin exposure, we performed chilled sucrose density centrifugation of D23580 to separate elongated from nonelongated bacteria. The untreated D23580 bacteria formed a single diffuse fraction at approximately 50% sucrose, whereas the bacteria treated with 2× MIC ciprofloxacin segregated into three smaller fractions (within 50%, 60%, and at the 60% to 70% sucrose interface) (Fig. 5; see also Data File S3 at https://doi.org/10.17605/OSF.IO/N9CW5). Based on our ability to separate morphologically distinct bacteria into specific fractions by density, we determined that there were meaningful subpopulations that formed in response to ciprofloxacin exposure. RNA sequencing of the three fractions generated with 2× MIC ciprofloxacin yielded markedly different transcriptional profiles. The low-density (50% sucrose) and high-density (60% sucrose) bacteria after 2× MIC ciprofloxacin exposure clustered independently with respect to their transcriptional profiles, which were also distinct from those of untreated bacteria (Fig. 5A; see also Tables S5 to S8).

An analysis of the top upregulated and downregulated genes showed that >100 genes were downregulated in the high-density compared to expression in the low-density ciprofloxacin-treated bacteria (Fig. 5B and c). Specifically, fewer genes were upregulated in the high-density fraction than in the low-density fractions of the ciprofloxacin-treated bacteria. We observed that *Salmonella* pathogenicity island 1 (SPI-1) and other invasion-associated genes were downregulated in the high-density ciprofloxacin-treated bacteria. In contrast, there was significant upregulation of some SPI-1 and SPI-2 genes in the low-density (50% sucrose) ciprofloxacin-treated bacteria compared to that in untreated bacteria (Fig. 5B and C; Tables S5 to S8). These data suggest that under ciprofloxacin treatment, elongated bacteria suppress genes that trigger cellular invasion and have an elevated stress response compared to that of nonelongated bacteria; additionally, the data suggest that ciprofloxacin-treated nonelongated bacteria may be better primed for cellular invasion and replication.

Ciprofloxacin exposure impacts host-pathogen interactions. We observed that ciprofloxacin-exposed D23580 downregulates SPI-1 and SPI-2 genes, suggesting that ciprofloxacin may impact the ability of *S.* Typhimurium to invade and replicate in host cells. Therefore, we tested this hypothesis by assessing the interaction between ciprofloxacin-exposed D23580 with macrophages and epithelial cells using a modified gentamicin protection assay (35, 36). To this end, bacteria were cultured for 2 h in the absence or presence of 0.06 μg/ml ciprofloxacin and subsequently inoculated onto monolayers of macrophages or HeLa cells. At 1.5 h postinfection, a significantly larger percentage of the ciprofloxacin-treated inoculum were internalized by macrophages (mean percent internalized of inoculum: 6.72% versus 1.50%, $P < 0.005$) (Fig. 6A, left). This difference is significant given that the inoculum added to cells, as measured by CFU/ml, was 100-fold lower for the ciprofloxacin-treated bacteria given 2 h of ciprofloxacin exposure (2.83E+06 ± 1.15E+06 CFU/ml for untreated bacteria versus 1.63E+04 ± 4.62E+03 CFU/ml for ciprofloxacin-treated bacteria). Thus, although significantly fewer ciprofloxacin-treated bacteria were added to equivalent numbers of macrophages, a significantly higher percentage of treated bacteria were internalized. Furthermore, the ciprofloxacin-treated bacteria had a higher replication rate in macrophages than untreated bacteria at 6 h postinfection (mean fold replication over

FIG 3 Legend (Continued)

Differential gene expression was analyzed using DESeq2. The relative expression (log2 fold change) of each gene for 2× MIC ciprofloxacin versus 0× MIC ciprofloxacin was calculated for each isolate, and genes with an adjusted *P* value of <0.05 were plotted along the chromosome. Genes with a $\log_2$ fold change of ≥2 are colored blue, and genes with a $\log_2$ fold change of ≤−2 are colored red to highlight highly differentially expressed genes.

TABLE 2 Top 20 significantly upregulated genes found commonly between SL1344, D23580, and VNS20081[a]

		SL1344		D23580		VNS20081	
Gene	Function	log_2fc	P_{adj}	log_2fc	P_{adj}	log_2fc	P_{adj}
recN	SOS response	3.99	0	3.75	0	3.38	3.97E−134
sulA	SOS response	3.64	7.09E−108	3.54	2.1E−134	2.43	6.92E−22
recA	SOS response	3.31	0	3.46	0	2.66	1.78E−222
stdA	Fimbriae production	3.09	1.48E−06	2.68	3.74E−09	5.60	1.17E−14
ilvC	Redox, biosynthesis	2.01	4.71E−52	2.51	2.29E−115	2.15	1.17E−37
uvrA	SOS response	2.30	0	2.38	1.87E−288	1.93	1.21E−71
lexA	SOS response	2.26	9.71E−150	2.28	9.69E−257	1.89	3.11E−160
cysJ	Redox, biosynthesis	2.10	2.27E−35	2.26	3.3E−22	1.74	1.51E−15
cysD	Redox, biosynthesis	1.60	6.24E−09	2.17	6.27E−26	1.44	7.44E−09
cysH	Redox, biosynthesis	1.76	5.51E−13	2.13	6.95E−25	1.20	0.00002
leuA	Biosynthesis	2.02	2.15E−20	2.08	2.7E−61	1.87	2.01E−13
cysI	Redox, biosynthesis	1.77	3.62E−28	2.00	4.66E−26	1.42	5.28E−10
cysC	Redox, biosynthesis	1.46	5.35E−09	1.94	1.57E−23	0.89	0.019
sodA	SOS response	1.47	2.83E−71	1.94	1.19E−194	1.48	4.4E−27
fadB	Redox, biosynthesis	1.28	2.41E−06	1.92	1.58E−18	1.99	4.79E−10
cpxP	Copper/H_2O_2 resistance	1.73	1.36E−24	1.86	2.44E−28	1.39	1.63E−14
polB	SOS response	2.27	2.24E−82	1.85	1.07E−42	1.80	1.13E−13
cysN	Redox, biosynthesis	1.65	9.53E−26	1.82	7.73E−29	0.85	0.0007
glmU	Biosynthesis	1.15	3.61E−110	1.80	3.87E−103	0.79	2.28E−23
fadA	Redox, biosynthesis	1.47	5.55E−06	1.79	9.25E−19	1.44	0.0007

[a]Differential expression analysis using DESeq2 was performed on each isolate independently for ciprofloxacin treatment versus no treatment, and only significant (adjusted *P* value [P_{adj}] < 0.05) log_2 fold change (log_2fc) results were included. The top 20 upregulated genes for D23580 were sorted in descending order by log_2fc and matched with corresponding log_2fc for SL1344 and VNS20081. A P_{adj} value of 0 indicates the value was so small that it was rounded to 0 by DESeq2.

1.5 h: 0.66 versus 0.20, $P < 0.05$) (Fig. 6A, right). It is possible that the macrophages internalized ciprofloxacin-treated bacteria at a higher rate because of their increased size and lower viability. However, this did not explain the greater intracellular survival and fold replication of ciprofloxacin-treated bacteria within macrophages.

To investigate whether the ciprofloxacin-treated bacteria were actively modulating interactions with host cells, the same assay was repeated using HeLa cells. We found that ciprofloxacin-treated D23580 bacteria displayed significantly lower rates of infection than untreated bacteria (mean percent internalized of inoculum: 0.44% versus 1.38%, $P < 0.005$) (Fig. 6B, left). However, in a comparable manner to that in macrophages, the fold replication 6 h postinfection of ciprofloxacin-treated bacteria was significantly higher than that of the untreated bacteria (mean fold replication over 1.5 h, 62.14 versus 7.88, $P < 0.05$) (Fig. 6B, right). This observation suggests that ciprofloxacin exposure diminishes invasion rates of epithelial cells but makes intracellular replication more efficient.

We hypothesized that debris from bacteria killed by ciprofloxacin may influence bacterial uptake by host cells. To assess whether the cultures of untreated and ciprofloxacin-treated bacteria differed, transmission electron microscopy (EM) was performed on the two cultures prior to infection (Fig. 6C). Using a negative stain, we observed that some ciprofloxacin-treated bacteria appeared to be associated with extracellular matter of unknow origin (Fig. 6C, bottom, inset). We could not identify substantial differences in the cultures of untreated and ciprofloxacin-treated bacteria, but further study may be warranted to determine whether ciprofloxacin-killed bacteria influence the survival of live bacteria in the same environment.

To determine whether the bacterial morphology influenced invasion of HeLa cells, bacteria were imaged immediately following the 30-min infection and at 1.5 h, following 1-h gentamicin treatment (Fig. 6D). At 30 min postinfection, there were elongated and nonelongated ciprofloxacin-treated bacteria extracellularly (Fig. 6D, top right). In contrast, imaging at 1.5 h postinfection showed similarly sized and shaped untreated and ciprofloxacin-treated internalized bacteria in HeLa cells (Fig. 6D, bottom row). Our

TABLE 3 Top 20 significantly downregulated genes found commonly between SL1344, D23580, and VNS20081[a]

		SL1344		D23580		VNS20081	
Gene	Function	log_2fc	P_{adj}	log_2fc	P_{adj}	log_2fc	P_{adj}
flgH	Flagellum	−2.17	2.16E−27	−2.60	7E−80	−2.52	7.39E−10
flgE	Flagellum	−1.83	4.78E−30	−2.58	1.06E−104	−2.42	4.77E−12
flgJ	Flagellum	−2.00	6.12E−21	−2.53	2.42E−79	−2.23	1.8E−15
flgF	Flagellum	−2.00	2.90E−25	−2.52	1.17E−77	−2.47	9.24E−10
flgG	Flagellum	−2.12	3.23E−33	−2.49	5.77E−95	−2.28	1.2E−09
flgI	Flagellum	−1.97	1.54E−20	−2.38	1.4E−62	−2.31	6.41E−15
flgC	Flagellum	−1.42	1.37E−17	−2.37	3.11E−76	−1.90	3.51E−08
flgB	Flagellum	−1.67	7.61E−25	−2.35	1.24E−61	−2.06	1.11E−14
fliO	Flagellum	−1.29	1.72E−11	−2.33	3.05E−44	−1.62	0.0000014
flgL	Flagellum	−1.53	2.72E−20	−2.28	4.34E−55	−2.30	1.9E−24
yciH	Putative translation factor	−1.38	8.11E−05	−2.28	1.06E−22	−1.66	0.0000188
flgK	Flagellum	−1.44	4.35E−22	−2.24	5.2E−98	−2.40	1.42E−27
flgM	Flagellum	−1.62	1.25E−14	−2.07	1.58E−25	−2.52	5.73E−18
yeeF	Putative transporter	−1.46	4.07E−172	−1.95	2.43E−242	−1.43	4.36E−103
fliN	Flagellum	−1.20	4.90E−10	−1.92	2.43E−39	−1.79	5.03E−12
fliI	Flagellum	−0.98	1.41E−11	−1.92	5.11E−09	−1.87	1.86E−14
ybiN	Conserved hypothetical protein	−1.80	5.83E−15	−1.91	3.86E−39	−1.16	0.000000294
fliL	Flagellum	−1.11	1.67E−14	−1.87	5.92E−46	−1.47	0.00000177
flgN	Flagellum	−1.59	2.12E−13	−1.83	9.32E−21	−1.88	2.25E−16
nth	Biosynthesis	−1.52	6.14E−14	−1.82	1.17E−32	−1.96	5.07E−08

[a]Differential expression analysis using DESeq2 was performed on each isolate independently for ciprofloxacin treatment versus no treatment, and only significant (adjusted *P* value [P_{adj}] < 0.05) log2 fold change (log_2fc) results were included. The top 20 downregulated genes for D23580 were sorted in ascending order by log_2fc and matched with corresponding log_2fc for SL1344 and VNS20081. A P_{adj} value of 0 indicates the value was so small that it was rounded to 0 by DESeq2.

data suggest that nonelongated ciprofloxacin-treated bacteria are more efficient than elongated ciprofloxacin-treated bacteria at invading HeLa cells, and it is possible that invasion by this subpopulation may enhance intracellular survival and replication.

DISCUSSION

Here, we investigated morphological and transcriptional responses of three distinct *S.* Typhimurium isolates against measured inhibitory concentrations of ciprofloxacin. We found that these bacteria were highly resilient to increasing concentrations of ciprofloxacin and adapt to this environment over a 24-h period of antimicrobial exposure, forming morphologically and transcriptionally distinguishable subpopulations early after exposure that have enhanced capacity to invade cells and replicate. Importantly, these data better define how clinical isolates respond to ciprofloxacin exposure, illustrating the potential for clinical *S.* Typhimurium isolates to tolerate and even replicate in the presence of concentrations of ciprofloxacin that should be fatal.

Ciprofloxacin (and other fluoroquinolones) are known to upregulate the bacterial stress response and phage activity (confirmed here), and the widespread use of ciprofloxacin is likely exacerbating AMR (18, 37). While population heterogeneity has been observed in response to ciprofloxacin exposure, past studies have used subinhibitory concentrations of ciprofloxacin against *Escherichia coli* (38, 39). Our work shows that subinhibitory concentrations of ciprofloxacin have a muted effect on the bacterial response and may be less relevant for understanding the bacterial response to clinical dosages. However, previous observations are in concordance with our findings that bacterial subpopulations have highly distinct transcriptional responses, which may imply a bet-hedging strategy to improve survival potential. Importantly, we also showed that the response to ciprofloxacin is specific and dosage dependent, and the upregulation of stress response and error-prone DNA replication machinery may influence bacterial survival and mutation (40–44). One limiting aspect of our study was that we did not longitudinally follow the bacterial response to ciprofloxacin, and future studies should also explore whether the ciprofloxacin MIC changes within a short time frame and how that affects the transcriptional response.

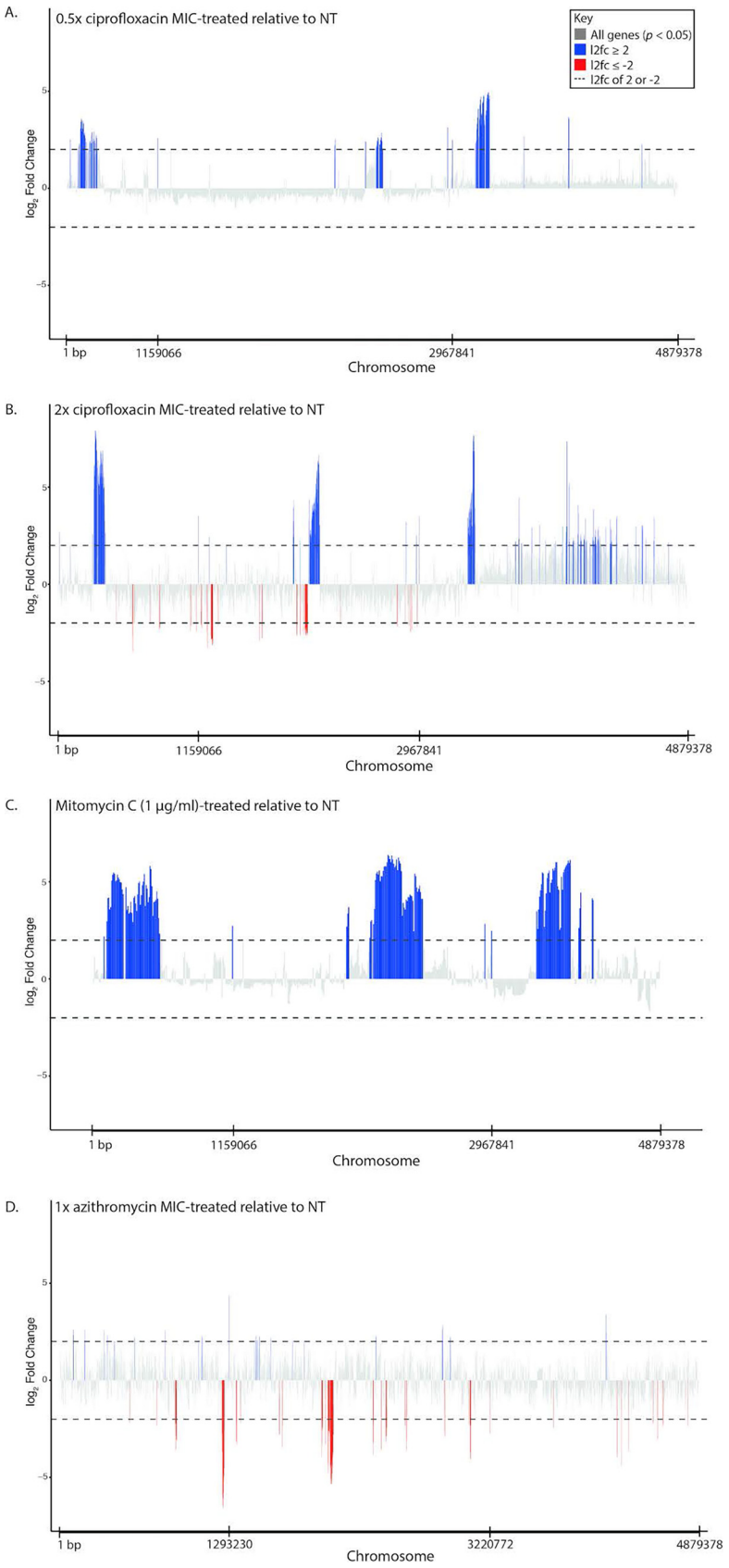

FIG 4 Bulk transcriptomics of *S.* Typhimurium D23580 under 4 different perturbations. *S.* Typhimurium D23580 was grown for 2 h in medium containing 0.5× ciprofloxacin MIC (A), 2× ciprofloxacin MIC (B),

(Continued on next page)

While not explored in this study, other groups have studied bacterial persistence in relation to ciprofloxacin at length (45–49). Bacterial persistence may factor into observations made in this study; however, one critical difference is that bacteria were consistently, rather than intermittently, exposed to ciprofloxacin. The ability of the bacteria to grow under constant ciprofloxacin pressure and subsequently invade host cells suggests additional factors are involved in cellular survival and resilience to ciprofloxacin during exposure.

Our work additionally suggests that ciprofloxacin-treated bacteria have somewhat different infection dynamics than untreated bacteria, which may have broader implications for patients on fluoroquinolone treatment. The invasion of, and replication within, HeLa cells and macrophages by *S.* Typhimurium has been well characterized, and many pathways involved in efflux and drug resistance have also been studied in the context of host-pathogen interactions (50, 51). Work by Anuforom et al. (52) found that J774 murine macrophages expressed greater concentrations of interleukin 1 beta (IL-1β) and tumor necrosis factor alpha (TNF-α) when pretreated with ciprofloxacin in the presence of SL1344. Additionally, they observed greater bacterial adhesion to ciprofloxacin-treated macrophages, resulting in enhanced bacterial killing (52). One limitation of our study is that we did not compare bacteria pretreated with ciprofloxacin to those exposed to ciprofloxacin within host cells. Given the findings of Anuforom et al. (52) and the importance of intracellular survival, intracellular interactions with ciprofloxacin may play a key role in drug evasion, and future work should investigate the response of *S.* Typhimurium to ciprofloxacin after cellular internalization.

However, in our study, we focused on the extracellular impacts of ciprofloxacin exposure, and the influence of ciprofloxacin treatment on bacteria prior to the infection of epithelial cells and macrophages has not been extensively studied. While we observed differences in the infection and replication potential between ciprofloxacin-treated and untreated *S.* Typhimurium that associated with transcriptional changes occurring in bacterial subpopulations, we did not investigate specific loci that could be responsible for the observed phenotype. It would be valuable to investigate any potential role in ciprofloxacin escape at the gene level to better understand how ciprofloxacin treatment may further affect *Salmonella* infections.

In a climate of mass drug administration (MDA) in parts of the world, it is particularly important to be aware of and actively study how bacteria respond to widespread antimicrobial exposure. In recent years, MDA studies have included single-dose administration of ciprofloxacin to combat *Neisseria meningitidis* in young children in the "meningitis belt" of Africa, prophylactic azithromycin in Niger, Malawi, and Tanzania to reduce childhood mortality, and azithromycin administration for children with nonbloody diarrhea in low-resource settings (53–55). While initial follow-up studies into resulting AMR have been performed, more genotypic and phenotypic surveillance is required (56). The potential for ciprofloxacin to trigger adaptive and genetic resistance in bacteria that may improve bacterial survival intracellularly provides impetus for greater caution in fluoroquinolone usage and more detailed investigation of the effect of ciprofloxacin and other antimicrobials on host-pathogen interactions.

MATERIALS AND METHODS

Bacterial isolates and growth medium. Three *Salmonella* Typhimurium isolates were used: SL1344 (ST19, United Kingdom), VNS20081 (ST34, Vietnam), and D23580 (ST313, Malawi) (22, 23, 57). Prior to experimentation, all isolates were grown on Iso-Sensitest agar (Oxoid, CM0471) and subjected to M.I.C.E. (Oxoid, MA0104F) ciprofloxacin eTests in duplicates to determine baseline ciprofloxacin susceptibility, and MIC range was confirmed by assessment on the Vitek2 (Table 4). Isolates were grown in Iso-

FIG 4 Legend (Continued)
1 μg/ml mitomycin C (C), or 1× azithromycin MIC (D) and subjected to RNA sequencing. Differential gene expression was analyzed using DESeq2. The relative expression ($\log_2$ fold change) of each gene for treatment versus no treatment was calculated for each condition, and genes with an adjusted *P* value of <0.05 were plotted along the chromosome. Genes with a $\log_2$ fold change of ≥ 2 are colored blue, and genes with a $\log_2$ fold change of ≤ -2 are colored red to highlight highly differentially expressed genes.

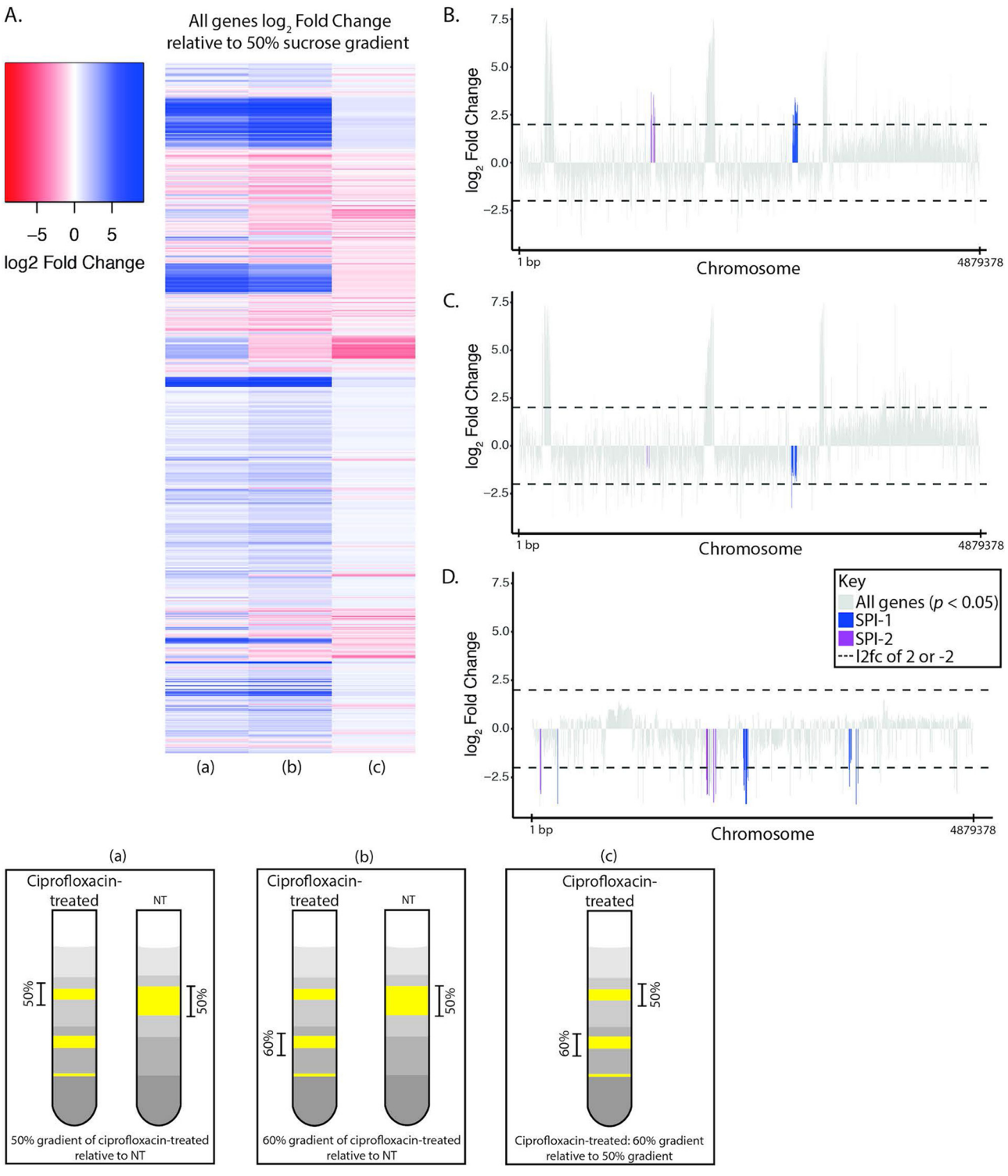

FIG 5 Transcriptomics of density gradient-separated *S.* Typhimurium D23580. *S.* Typhimurium D23580 was grown for 2 h in either 0× (NT) or 2× MIC ciprofloxacin and layered on sucrose gradients containing 25%, 50%, 60%, and 70% sucrose layers. Following density centrifugation, gradient-separated bacteria were subjected to RNA sequencing, and differential gene expression was analyzed using DESeq2. (A) Three comparisons were performed, and the $\log_2$ fold change of relative gene expression was plotted as a heat map with upregulated genes in blue and downregulated genes in red. The comparisons were ciprofloxacin-treated 50% sucrose gradient versus NT (a), ciprofloxacin-treated 60% sucrose gradient versus NT (b), and ciprofloxacin-treated 60% sucrose gradient versus ciprofloxacin-treated 50% sucrose gradient (c). (B) For the comparison of ciprofloxacin-treated 50% sucrose gradient versus NT, significantly differentially expressed ($P < 0.05$) genes were plotted along the chromosome, and genes found within SPI-1 and SPI-2 are colored purple and blue, respectively. (C) The comparison of ciprofloxacin-treated 60% sucrose gradient versus NT was mapped along the chromosome as for panel B. (D) The comparison of ciprofloxacin-treated 60% sucrose gradient versus ciprofloxacin-treated 50% sucrose gradient as in panel B.

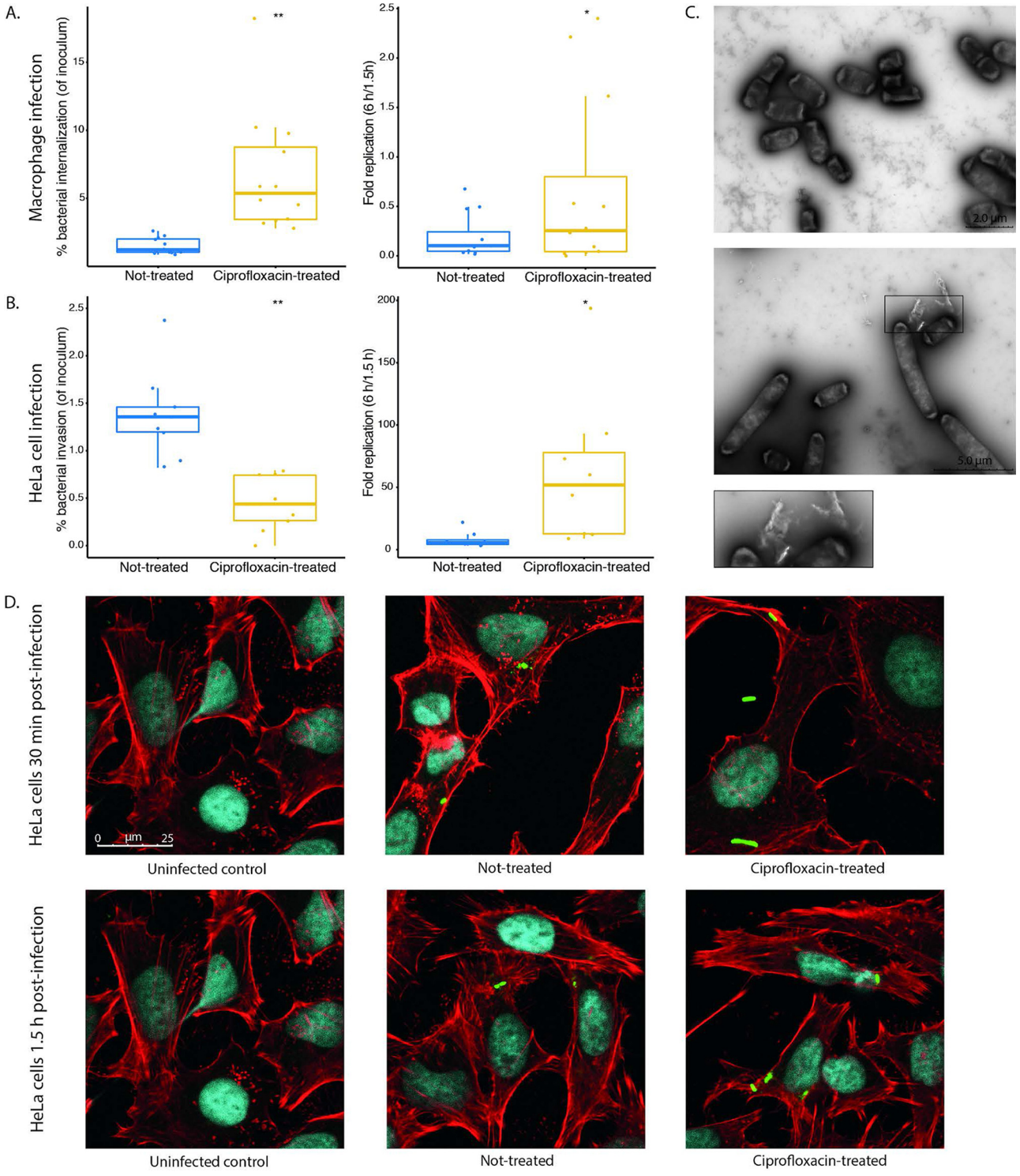

FIG 6 Cellular infections with *S.* Typhimurium D23580 following 2 h of ciprofloxacin exposure. *S.* Typhimurium D23580 was either not treated or treated with 2× MIC ciprofloxacin for 2 h prior to infection of macrophages (A) or HeLa cells (B). (Left) Bacterial internalization 1.5 h postinfection. (Right) Bacterial intracellular replication 6 h postinfection. Boxplots represent the means and interquartile ranges from four (macrophages) or three (HeLa cells) biological replicates of three technical replicates each. The means and SDs were calculated, and a Student's paired *t* test was performed to calculate significance. *, $P < 0.05$; **, $P < 0.005$. (C) Transmission electron microscopy was performed using negatively stained D23580 either not treated (top panel) or treated with 2× MIC ciprofloxacin (bottom) for 2 h. Box inset shows extracellular matter in ciprofloxacin-treated culture. (D) Confocal images were taken of D23580 either not treated or treated with 2× ciprofloxacin MIC immediately following the initial 30-min infection of HeLa cells (top) or after the subsequent 1-h gentamicin treatment (bottom). HeLa cell membranes were stained with phalloidin (red), nucleic acids were stained with DAPI (blue), and bacteria were stained with CSA (green). Images of infected cells are compared to an uninfected control image for reference (left, same image used as comparator for 30 min and 1.5 h).

TABLE 4 MICs using Vitek 2 and ciprofloxacin eTest

Strain	MIC (μg/ml)	
	Vitek2 ciprofloxacin result	M.I.C.E. ciprofloxacin eTest result
D23580	≤0.25	0.03
SL1344	≤0.25	0.015
VNS20081	2	1

Sensitest broth (Oxoid, CM0473) for all except host cell experiments and were maintained on Iso-Sensitest agar and streaked weekly from frozen stocks.

Time-kill curves. Colonies from plates were inoculated in 10 ml Iso-Sensitest broth for 16 to 18 h shaking at 200 rpm at 37°C. Bacteria were added in a 1:10,000 dilution to 10 ml of Iso-Sensitest containing levels (0×, 1×, 2×, and 4× MIC) of ciprofloxacin according to each isolate's MIC for an inoculum of between 1 and 5×10^5 CFU/ml. Cultures were incubated shaking at 37°C, and aliquots were taken for CFU plating at 0, 2, 4, 6, 8, and 24 h. Serial dilutions were made, and a total of 50 μl of each dilution was plated in 10 μl on L agar. CFU were counted and calculated as CFU per milliliter. Means and standard deviations (SDs) from three replicates per isolate were calculated. Log_{10} CFU per milliliter values were plotted over 24 h as three independent replicates, with the color indicating the growth condition (0×, 1×, 2×, and 4× ciprofloxacin MIC) in R using ggplot2 (58, 59). To compare mean CFU per milliliter values for the 24-h time point, an analysis of variance (ANOVA) was performed, and statistical significance of differences in the means of conditions compared to that for 0× (control) were conducted using Dunnett's test.

Ciprofloxacin-degradation kill curves. Initial 24 h time-kill curves were performed as described above. At 24 h, cultures were centrifuged and sterile filtered, and filtered medium was transferred to fresh tubes. As described above, overnight cultures were added 1:10,000 to the medium and CFU were plated at 0, 2, 4, 6, 8, and 24 h. No additional ciprofloxacin was added to the medium.

RNA extractions and RNA sequencing. After bacteria were subcultured at 1:1,000 for 2 h in the presence or absence of 2× ciprofloxacin MIC, double the quantity of RNAprotect bacteria reagent (Qiagen, 76506) was added to cultures and incubated for 10 min. Cultures were centrifuged at 3,215 × *g* for 14 min at 4°C. Supernatant was decanted and resuspended in 400 μl Tris buffer (0.25 mM, pH 8.0) containing 10 mg/ml lysozyme and incubated for 5 min. To this, 700 μl RLT buffer containing 10 μl/ml beta-mercaptoethanol (Sigma, M6250) was added and vortexed well. One milliliter 100% ethanol was immediately added and vortexed well. The Qiagen RNeasy minikit (Qiagen, 74104) was subsequently used to process samples. Samples were eluted in 40 μl RNase-free water. Samples were frozen at −20°C if not immediately processed. Subsequently, samples were treated with DNase I using the Qiagen DNase kit (Qiagen, 79254). Output following DNase treatment was cleaned using phenol-chloroform treatment by first increasing the solution volume with RNase-free water to 400 μl. Four hundred microliters of phenol-chloroform-isoamyl alcohol mixture (Sigma, 77617) was added to samples, which were mixed by inversion and then centrifuged at 8,000 × *g* for 5 min. The supernatant was transferred to a new tube and combined with 400 μl chloroform-isoamyl alcohol (24:1) (Sigma, C0549). Samples were mixed and then centrifuged as described above. The supernatant was transferred to a new tube and combined with 1 μl glycogen (Roche, 10901393001), 40 μl 3 M sodium acetate, pH 5.5 (Ambion, AM9740), and 500 μl ice-cold 100% ethanol. Tubes were mixed by inversion and incubated at −20°C for 30 min before centrifugation at 4°C for 20 min at 16,000 × *g*. Supernatant was decanted, replaced with 500 μl ice-cold 70% ethanol, and centrifuged at 4°C for 5 min at 16,000 × *g*. Ethanol was decanted and pellets were air dried before resuspension in 50 μl RNase-free water. Samples were frozen at −80°C prior to sequencing.

All library preparation and RNA sequencing were performed at the Wellcome Sanger Institute using standard protocols. Briefly, libraries were made using the NEB Ultra II RNA custom kit (NEB, E7530S) on an Agilent Bravo WS automation system. RiboZero was added to deplete rRNA. Libraries were pooled and normalized to 2.8 nM for sequencing. Sequencing was performed on an Illumina HiSeq 4000 (Illumina, San Diego, CA), using a minimum of two lanes per pool.

RNA sequencing analysis. Reads from D23580 were mapped to reference sequence D23580 (accession number FN424405.1) (22), VNS20081 was mapped to sequence VNB151 (accession number ERS745838) (23), and SL1344 was mapped to reference sequence SL1344 (accession number FQ312003.1). Sanger Institute pipeline DEAGO (Differential Expression Analysis & Gene Ontology), a wrapper script for DESeq2 and topGO (60, 61), was used to determine differential gene expression. Using DESeq2, a Wald test was conducted on the treatment condition versus untreated. The $\log_2$ fold change was calculated for treatment condition versus untreated after filtering genes to include only those with an adjusted *P* value (P_{adj}) of <0.05 to control for the false-discovery rate using the Benjamini-Hochberg procedure. All differential expression analyses were conducted using default DESeq2 parameters (60). Genes that had a P_{adj} of <0.05 and a $\log_2$ fold change of ≥2 or ≤−2 were subjected to further manual analysis to assess top up- and downregulated genes in treatment conditions relative to expression in those that were untreated. Visualization of differentially expressed genes was performed using the ggplot2 package in R.

Sucrose gradient separation of ciprofloxacin-treated D23580. To separate morphologically distinct subpopulations of bacteria after ciprofloxacin exposure, a sucrose gradient procedure was developed. Overnight cultures of D23580 were grown as described above, inoculated 1:100 into 10 ml of Iso-

Sensitest broth containing either 0 or 0.06 μg/ml ciprofloxacin, and incubated shaking at 200 rpm at 37°C for 2 h. Fresh sucrose solutions were prepared: the four concentrations of sucrose used were 25%, 50%, 60%, and 70%, and these were made by dissolving sucrose (Sigma, S7903) in 1× phosphate-buffered saline (PBS). Solutions were sterile filtered using 0.2-μm syringe filters (GE Healthcare, 6794-2502). Two milliliters of each sucrose concentration was layered from 70% to 25% in open-top ultracentrifuge tubes (Beckman Coulter, 344059) immediately before use. At 2 h, cultures were removed from the incubator and centrifuged in a benchtop swing bucket centrifuge for 14 min at 4,000 × *g* at 4°C. The supernatant was removed with a pipette. Pellets were resuspended in the remaining medium and transferred to 1.5-ml tubes, which were centrifuged at 5,000 × *g* for 2 min to repellet. The supernatant was removed, and pellets were resuspended in 500 μl PBS. Using a Pasteur pipette, 500 μl of cells was carefully added to the top of the 25% layer of the sucrose column. Gradients were centrifuged for 9 min at 3,000 × *g* at 4°C. After centrifugation, gradients were identified as follows:

- one layer on the gradients loaded with nontreated cultures within the 50% sucrose fraction
- three layers from the 2× MIC ciprofloxacin-treated gradients, (i) within 50%, (ii) within 60%, and (iii) 60% to 70% interface.

The cloudy portion of each layer was carefully removed using a Pasteur pipette, beginning with the lowest-density layer, and isolated fractions were immediately added to 10 ml bacterial RNAprotect and processed using the standard RNA extraction protocol described above.

RNA sequencing analysis of gradient-separated bacteria. RNA sequencing (RNA-seq) analysis was performed on the bacteria recovered from the gradients. These RNA sequencing reads were processed using DEAGO. Pairwise comparisons were made between conditions (ciprofloxacin-treated 50% versus untreated 50%, ciprofloxacin-treated 60% versus untreated 50%, and ciprofloxacin-treated 60% versus ciprofloxacin-treated 50%). Heat maps were made using the heatmap.2 function in R package gplots, and other visualizations were performed using ggplot2.

DNA extraction of 24-h ciprofloxacin-treated cultures. To prepare DNA, bacterial cultures of *S.* Typhimurium D23580 were initially grown overnight in 10 ml of broth. As in the time-kill curve experiments, 10 ml of fresh Iso-Sensitest broth containing no or 0.06 μg/ml ciprofloxacin MIC was inoculated with overnight cultures at 1:10,000. Bacteria were grown for 24 h before spreading 100 μl or 1,000 μl for the untreated and ciprofloxacin-treated cultures, respectively, on L agar plates. Plates were grown overnight to ensure only DNA from viable organisms was sequenced as a plate sweep (62). After overnight growth at 37°C, colonies were scraped from the agar and resuspended in 1× PBS. This was spun down at 8,000 rpm for 3 min, and the supernatant was aspirated off. The pellets were processed for DNA extraction using the Promega Wizard DNA purification kit (Promega, A1120). DNA was quantified on a Qubit 4 fluorometer (Q33226) using the Qubit double-stranded DNA (dsDNA) HS assay kit (Q32851) and then frozen at −80°C prior to whole-genome sequencing. DNA was sequenced on an Illumina HiSeq platform. Illumina adapter content was trimmed from reads using Trimmomatic v.0.33.

Read mapping and variant detection of 24-h ciprofloxacin-treated cultures. Illumina HiSeq reads were mapped to *S.* Typhimurium reference genome D23580 (FN424405.1) using SMALT v0.7.4 to produce a BAM file. Briefly, variant detection was performed as previously detailed (63). SAMtools mpileup v0.1.19 with parameters -d 1000 -DSugBf and bcftools v0.1.19 were used to generate a BCF file of all variant sites. The bcftools variant quality score was set as greater than 50, mapping quality was set as greater than 30, the allele frequency was determined as either 0 for bases called same as the reference or 1 for bases called as a SNP (af1 $<$ 0.95), the majority base call was set to be present in at least 75% of reads mapping at the base (ratio $<$ 0.75), the minimum mapping depth was four reads, a minimum of two of the four had to map to each strand, and strand_bias was set as less than 0.001, map_bias less than 0.001, and tail_bias less than 0.001. Bases that did not meet those criteria were called uncertain and removed. A pseudogenome was constructed by substituting the base calls in the BCF file in the reference genome. Recombinant regions in the chromosome such as prophage regions were removed from the alignment and checked using Gubbins v1.4.10. SNP sites were extracted from the alignment using snp-sites and analyzed manually.

Opera Phenix confocal microscopy phenotyping of single bacteria. *S.* Typhimurium D23580, SL1344, and VNS20081 were screened at 2 h after ciprofloxacin exposures of 0×, 1×, 2×, and 4× as related to the MIC of the isolate. This was undertaken by inoculating overnight cultures independently at 1:1,000 dilutions of 150 μl in 150 ml Iso-Sensitest broth in a 200-ml flask and incubated with shaking. Following 2 h of growth, 10 ml of each culture was spun down at 3,200 × *g* for 7 min at 4°C. The supernatant was decanted, and the pellet was transferred to a 1.5-ml tube. This was spun at 8,000 × *g* for 3 min, and the supernatant was decanted and replaced with 100 μl PBS. For each culture condition, 50 μl of the concentrated bacterial culture was added to two wells of a vitronectin-coated Opera CellCarrier Ultra-96 plate (Perkin Elmer, 6055302), and the plates were incubated static at 37°C for 10 min. The microbial culture was aspirated, fixed with 4% paraformaldehyde (PFA), and washed with 1× PBS. Wells were incubated with 2% bovine serum albumin (BSA) for 30 min and then for 1 h with CSA-Alexa Fluor 647 (Novus Biologicals, NB110-16952AF647) at 1:1,000 in BSA. Wells were aspirated and then incubated with solutions harboring 4′,6-diamidino-2-phenylindole (DAPI) (Invitrogen, D1306) and SYTOX green (Invitrogen, S7020) for 20 min. Wells were washed 1× with PBS; plates were sealed and imaged.

Opera Phenix confocal microscopy image analysis of single bacteria. Images generated on the Opera Phenix were analyzed using the Harmony software (Perkin Elmer), as previously described (24, 65). Briefly, inputted images underwent flatfield correction, and images were calculated using the DAPI and Alexa Fluor 647 channels and then refined by size and shape characteristics. Applying a linear classifier to the filtered population, single bacteria were identified, and morphology and intensity

characteristics were calculated. The output of the Harmony analysis was tabulated by object, and results were visualized in R (v 3.6.1) using R packages dplyr and ggplot2.

HeLa cell and iPS macrophage infections with *S.* Typhimurium D23580. HeLa cells were obtained from Abcam (ab255928) and maintained in Dulbecco's modified Eagle medium (DMEM) (Thermo, 41966) supplemented with 10% heat-inactivated fetal bovine serum (FBS) (Merck, F7524) incubated at 37°C with 5% CO_2. HeLa cells were plated in 24-well plates (Corning, 3473) at 1×10^5 cells/ml in 500 μl medium. D23580 was inoculated from a freshly streaked plate in 10 ml LB and incubated shaking overnight at 37°C the day prior to infections. On the day of infections, two D23580 subcultures were set up 1:10 in LB from the overnight culture, with one subculture containing 0.06 μg/ml of ciprofloxacin. Cultures were incubated with shaking at 37°C for 2 h. At 2 h, the optical density at 600 nm (OD_{600}) of cultures was measured, and bacteria were resuspended in PBS after normalization to an OD_{600} of 1.0. Bacteria were added to cell medium for a multiplicity of infection of ~10:1. Five hundred microliters of the inoculum was added to each well and incubated for 30 min. The inoculum was plated for CFU enumeration. Following the infection, medium was aspirated and cells were washed 1× with PBS. PBS was replaced with medium containing 16 μg/ml gentamicin (Gibco, 15750037), and plates were incubated for 1 h. Medium was aspirated, and plates were washed 1× with PBS which was subsequently replaced with either 0.1% Triton-X for the 1.5-h time point or medium until 6 h postinfection. To enumerate CFU, 100 μl of cell lysates was spread on L agar plates, and plates were incubated overnight at 37°C before counting. The same process was followed at 6 h postinfection. Infections were conducted in technical triplicates.

Macrophages derived from induced pluripotent stem (iPS) cells were produced as previously described (64). Monocytes in RPMI containing human macrophage colony-stimulating factor (hMCSF) cytokine (Bio Techne/216-MC-025) were plated in 24-well plates at 1.5×10^5 7 days prior to infection, and the medium was changed to RPMI without hM-CSF 1 day prior to infection. Cells were infected with D23580 as described above for HeLa cells, and CFU were enumerated.

Confocal microscopy of infected HeLa cells. HeLa cells (1×10^5 cells/ml) were added to coverslips (Thermo, 12392128) in 24-well plates, and infections with D23580 were conducted as described above. After the 30-min infection, one set of coverslips was immediately fixed in 4% PFA without washing to image intracellular and extracellular bacteria. The remaining coverslips were processed as CFU wells and fixed at 1.5 h postinfection. Coverslips were blocked and permeabilized using 250 μl 10% BSA plus 0.1% Triton X-100 in PBS for 15 min at room temperature. CSA (BacTrace, 5330-0059) and phalloidin (A22287) antibodies were diluted in 1% BSA plus 0.1% Triton X-100 in PBS at 1:100 and 1:1,000, respectively. Two hundred fifty microliters of the CSA antibody was added first and incubated in the dark at room temperature for 1 h. Coverslips were washed 3× in 250 μl PBS, and then 250 μl of phalloidin was added to coverslips and incubated in the dark at room temperature for 1 h. Coverslips were washed 3× in 250 μl PBS. Coverslips were mounted on glass slides with 20 μl Prolong Gold with DAPI (Invitrogen, P36935) and cured in the dark at room temperature overnight. Twenty-five fields per coverslip were imaged on a Leica TCS SP8 confocal microscope at ×40 magnification.

Transmission electron microscopy of *S.* Typhimurium D23580. D23580 overnight cultures were added 1:10 to 10 ml LB containing either none or 0.06 μg/ml ciprofloxacin and incubated with shaking for 2 h. For staining, 1 ml of uranyl acetate (UA) solution (3% aqueous) was filter sterilized through a 0.2-μm filter. One 200-square mesh Cu EM grid (Agar Scientific) was spotted with 10 μl bacterial sample and left for 1 min. Filter paper was used to remove excess liquid, and 10 μl UA was added to the grid for 1 min. Excess liquid was again removed using filter paper, and the grid was allowed to dry for 1 h prior to imaging. Imaging was performed on a Hitachi HT7800 transmission electron microscope at 100 kV, 8 μA, and a range of magnifications.

Data availability. RNA sequencing reads can be found using the BioProject accession number PRJEB43116 (ERP127047). Whole-genome sequencing reads can be found using the accession number PRJEB43255 (ERP127204). Data File S1 (RNA-seq differential expression analysis results of *S.* Typhimurium isolates SL1344, D23580, and VNS20081), Data File S2 (RNA-seq differential expression analysis results of *S.* Typhimurium D23580 exposed to 4 parallel conditions), Data File S3 (RNA-seq differential expression analysis results of *S.* Typhimurium D23580 sucrose gradients), and Data File S4 (sample names and corresponding accession numbers for raw sequencing data stored in ENA) are available at https://doi.org/10.17605/OSF.IO/N9CW5.

SUPPLEMENTAL MATERIAL

Supplemental material is available online only.

FIG S1, DOCX file, 0.4 MB.

TABLE S1, DOCX file, 0.1 MB.

TABLE S2, DOCX file, 0.1 MB.

TABLE S3, DOCX file, 0.1 MB.

TABLE S4, DOCX file, 0.1 MB.

TABLE S5, DOCX file, 0.1 MB.

TABLE S6, DOCX file, 0.1 MB.

TABLE S7, DOCX file, 0.1 MB.

TABLE S8, DOCX file, 0.1 MB.

ACKNOWLEDGMENTS

This work was supported by Wellcome (grant 206194) and the Wellcome Sanger Institute (Ph.D. studentship to S.S.). S.B. is supported by a Wellcome senior research fellowship (215515/Z/19/Z). This work was supported by a Innovate UK Commercial in Confidence grant to purchase the Opera Phenix. S.F., S.B., C.C., D.P., and G.D. are supported by funding from the National Institute for Health Research (Cambridge Biomedical Research Centre at the Cambridge University Hospitals NHS Foundation Trust) and National Institute for Health Research AMR Research Capital Funding Scheme (NIHR200640).

The funders had no role in the design and conduct of the study, collection, management, analysis, and interpretation of the data, preparation, review, or approval of the manuscript, or decision to submit the manuscript for publication.

We thank Sina Beier for help with the RNA sequencing analysis and Sandra Van Puyvelde for helpful discussions during the project. We also thank the Wellcome Sanger Institute Sequencing Pipelines team for sequencing assistance and the Wellcome Sanger Institute Pathogen Informatics team for bioinformatics support.

REFERENCES

1. Tacconelli E, Carrara E, Savoldi A, Harbarth S, Mendelson M, Monnet DL, Pulcini C, Kahlmeter G, Kluytmans J, Carmeli Y, Ouellette M, Outterson K, Patel J, Cavaleri M, Cox EM, Houchens CR, Grayson ML, Hansen P, Singh N, Theuretzbacher U, Magrini N, WHO Pathogens Priority List Working Group. 2018. Discovery, research, and development of new antibiotics: the WHO priority list of antibiotic-resistant bacteria and tuberculosis. Lancet Infect Dis 18:318–327. https://doi.org/10.1016/S1473-3099(17)30753-3.
2. O'Neill J. 2016. Tackling drug-resistant infections globally: final report and recommendations. Review on antimicrobial resistance, London, United Kingdom.
3. Walker RC, Wright AJ. 1991. The fluoroquinolones. Mayo Clin Proc 66:1249–1259. https://doi.org/10.1016/s0025-6196(12)62477-x.
4. Aldred KJ, Kerns RJ, Osheroff N. 2014. Mechanism of quinolone action and resistance. Biochemistry 53:1565–1574. https://doi.org/10.1021/bi5000564.
5. Wohlkonig A, Chan PF, Fosberry AP, Homes P, Huang J, Kranz M, Leydon VR, Miles TJ, Pearson ND, Perera RL, Shillings AJ, Gwynn MN, Bax BD. 2010. Structural basis of quinolone inhibition of type IIA topoisomerases and target-mediated resistance. Nat Struct Mol Biol 17:1152–1153. https://doi.org/10.1038/nsmb.1892.
6. Laponogov I, Sohi MK, Veselkov DA, Pan X, Sawhney R, Thompson AW, Mcauley KE, Fisher LM, Sanderson MR. 2009. Structural insight into the quinolone–DNA cleavage complex of type IIA topoisomerases. Nat Struct Mol Biol 16:667–669. https://doi.org/10.1038/nsmb.1604.
7. Zhang CZ, Ren SQ, Chang MX, Chen PX, Ding HZ, Jiang HX. 2017. Resistance mechanisms and fitness of *Salmonella* Typhimurium and *Salmonella* Enteritidis mutants evolved under selection with ciprofloxacin *in vitro*. Sci Rep 7:9113. https://doi.org/10.1038/s41598-017-09151-y.
8. Acheampong G, Owusu M, Owusu-Ofori A, Osei I, Sarpong N, Sylverken A, Kung HJ, Cho ST, Kuo CH, Park SE, Marks F, Adu-Sarkodie Y, Owusu-Dabo E. 2019. Chromosomal and plasmid-mediated fluoroquinolone resistance in human *Salmonella enterica* infection in Ghana. BMC Infect Dis 19:898. https://doi.org/10.1186/s12879-019-4522-1.
9. Garvey MI, Rahman MM, Gibbons S, Piddock LV. 2011. Medicinal plant extracts with efflux inhibitory activity against Gram-negative bacteria. Int J Antimicrob Agents 37:145–151. https://doi.org/10.1016/j.ijantimicag.2010.10.027.
10. Baucheron S, Coste F, Canepa S, Maurel MC, Giraud E, Culard F, Castaing B, Roussel A, Cloeckaert A. 2012. Binding of the RamR repressor to wild-type and mutated promoters of the *ramA* gene involved in efflux-mediated multidrug resistance in *Salmonella enterica* serovar Typhimurium. Antimicrob Agents Chemother 56:942–948. https://doi.org/10.1128/AAC.05444-11.
11. Ricci V, Peterson ML, Rotschafer JC, Wexler H, Piddock LV. 2004. Role of topoisomerase mutations and efflux in fluoroquinolone resistance of *Bacteroides fragilis* clinical isolates and laboratory mutants. Antimicrob Agents Chemother 48:1344–1346. https://doi.org/10.1128/aac.48.4.1344-1346.2004.
12. Dimitrov T, Udo EE, Albaksami O, Kilani AA, Shehab E-D. 2007. Ciprofloxacin treatment failure in a case of typhoid fever caused by *Salmonella enterica* serotype Paratyphi A with reduced susceptibility to ciprofloxacin. J Med Microbiol 56:277–279. https://doi.org/10.1099/jmm.0.46773-0.
13. Stevenson JE, Gay K, Barrett TJ, Medalla F, Chiller TM, Angulo FJ. 2007. Increase in nalidixic acid resistance among non-Typhi *Salmonella enterica* isolates in the United States from 1996 to 2003. Antimicrob Agents Chemother 51:195–197. https://doi.org/10.1128/AAC.00222-06.
14. Wannaprasat W, Padungtod P, Chuanchuen R. 2011. Class 1 integrons and virulence genes in *Salmonella enterica* isolates from pork and humans. Int J Antimicrob Agents 37:457–461. https://doi.org/10.1016/j.ijantimicag.2010.12.001.
15. Kloskowski T, Gurtowska N, Drewa T. 2010. Does ciprofloxacin have an obverse and a reverse? Pulm Pharmacol Ther 23:373–375. https://doi.org/10.1016/j.pupt.2010.02.005.
16. Patkari M, Mehra S. 2013. Transcriptomic study of ciprofloxacin resistance in *Streptomyces coelicolor* A3(2). Mol Biosyst 9:3101–3116. https://doi.org/10.1039/c3mb70341j.
17. Li L, Dai X, Wang Y, Yang Y, Zhao X, Wang L, Zeng M. 2017. RNA-seq-based analysis of drug-resistant *Salmonella enterica* serovar Typhimurium selected *in vivo* and *in vitro*. PLoS One 12:e0175234. https://doi.org/10.1371/journal.pone.0175234.
18. Wang X, Kim Y, Ma Q, Hong SH, Pokusaeva K, Sturino JM, Wood TK. 2010. Cryptic prophages help bacteria cope with adverse environments. Nat Commun 1:147. https://doi.org/10.1038/ncomms1146.
19. Machuca J, Recacha E, Briales A, Díaz-de-Alba P, Blazquez J, Álvaro P, Rodríguez-Martínez JM. 2017. Cellular response to ciprofloxacin in low-level quinolone-resistant *Escherichia coli*. Front Microbiol 8:1370. https://doi.org/10.3389/fmicb.2017.01370.
20. Huguet A, Pensec J, Soumet C. 2013. Resistance in *Escherichia coli*: variable contribution of efflux pumps with respect to different fluoroquinolones. J Appl Microbiol 114:1294–1299. https://doi.org/10.1111/jam.12156.
21. Yamane T, Enokida H, Hayami H, Kawahara M, Nakagawa M. 2012. Genome-wide transcriptome analysis of fluoroquinolone resistance in clinical isolates of *Escherichia coli*. Int J Urol 19:360–368. https://doi.org/10.1111/j.1442-2042.2011.02933.x.
22. Kingsley RA, Msefula CL, Thomson NR, Kingsley RA, Msefula CL, Thomson NR, Kariuki S, Holt KE, Gordon MA, Harris D, Clarke L, Whitehead S, Sangal V, Marsh K, Achtman M, Molyneux ME, Cormican M, Parkhill J, Maclennan CA, Heyderman RS, Dougan G. 2009. Epidemic multiple drug resistant *Salmonella* Typhimurium causing invasive disease in sub-Saharan Africa have a distinct genotype. Genome Res 19:2279–2287. https://doi.org/10.1101/gr.091017.109.
23. Mather AE, Phuong TLT, Gao Y, Clare S, Mukhopadhyay S, Goulding DA, Do Hoang NT, Tuyen HT, Lan NPH, Thompson CN, Trang NHT, Carrique-Mas J, Tue NT, Campbell JI, Rabaa MA, Thanh DP, Harcourt K, Hoa NT, Trung NV, Schultsz C, Perron GG, Coia JE, Brown DJ, Okoro C, Parkhill J, Thomson NR, Chau NVV, Thwaites GE, Maskell DJ, Dougan G, Kenney LJ, Baker S. 2018. New variant of multidrug-resistant *Salmonella enterica* serovar Typhimurium associated with invasive disease in immunocompromised patients in Vietnam. mBio 9:e01056-18. https://doi.org/10.1128/mBio.01056-18.
24. Maes M, Dyson ZA, Smith SE, Goulding DA, Ludden C, Baker S, Kellam P, Reece ST, Dougan G, Scott JB. 2020. A novel therapeutic antibody screening method using bacterial high-content imaging reveals functional antibody binding phenotypes of *Escherichia coli* ST131. Sci Rep 10:12414. https://doi.org/10.1038/s41598-020-69300-8.

25. Little JW, Edmiston SH, Pacelli LZ, Mount DW. 1980. Cleavage of the *Escherichia coli* lexA protein by the recA protease. Proc Natl Acad Sci U S A 77:3225–3229. https://doi.org/10.1073/pnas.77.6.3225.
26. Yim G, McClure J, Surette MG, Davies JE. 2011. Modulation of *Salmonella* gene expression by subinhibitory concentrations of quinolones. J Antibiot (Tokyo) 64:73–78. https://doi.org/10.1038/ja.2010.137.
27. Janion C. 2008. Inducible SOS response system of DNA repair and mutagenesis in *Escherichia coli*. Int J Biol Sci 4:338–344. https://doi.org/10.7150/ijbs.4.338.
28. Rushdy AA, Mabrouk MI, Abu-Sef FAH, Kheiralla ZH, All SMA, Saleh NM. 2013. Contribution of different mechanisms to the resistance to fluoroquinolones in clinical isolates of *Salmonella enterica*. Braz J Infect Dis 17:431–437. https://doi.org/10.1016/j.bjid.2012.11.012.
29. Villagra NA, Valenzuela LM, Mora AY, Millanao AR, Saavedra CP, Mora GC, Hidalgo AA. 2019. Cysteine auxotrophy drives reduced susceptibility to quinolones and paraquat by inducing the expression of efflux-pump systems and detoxifying enzymes in *S.* Typhimurium. Biochem Biophys Res Commun 515:339–344. https://doi.org/10.1016/j.bbrc.2019.05.122.
30. Hu WS, Chen H-W, Zhang R-Y, Huang C-Y, Shen C-F. 2011. The expression levels of outer membrane proteins STM1530 and OmpD, which are influenced by the CpxAR and BaeSR two-component systems, play important roles in the ceftriaxone resistance of *Salmonella enterica* serovar Typhimurium. Antimicrob Agents Chemother 55:3829–3837. https://doi.org/10.1128/AAC.00216-11.
31. Otsuji N, Sekiguchi M, Iijima T, Takagi Y. 1959. Induction of phage formation in the lysogenic *Escherichia coli* K-12 by mitomycin C. Nature 184:1079–1080. https://doi.org/10.1038/1841079b0.
32. Smith-Kielland I. 1966. The effect of mitomycin C on deoxyribonucleic acid and messenger ribonucleic acid in *Escherichia coli*. Biochim Biophys Acta 114:254–263. https://doi.org/10.1016/0005-2787(66)90307-8.
33. Levine M. 1961. Effect of mitomycin C on interactions between temperate phages and bacteria. Virology 13:493–499. https://doi.org/10.1016/0042-6822(61)90280-x.
34. Giacomoni PU. 1982. Induction by mitomycin C of recA protein synthesis in bacteria and spheroplasts. J Biol Chem 257:14932–14936. https://doi.org/10.1016/S0021-9258(18)33373-8.
35. Elsinghorst EA. 1994. Measurement of invasion by gentamicin resistance, p 405–420. *In* Clark VL, Bavoil PM (ed), Bacterial pathogenesis part B: interaction of pathogenic bacteria with host cells. Academic Press, Cambridge, MA.
36. Lee CA, Falkow S. 1990. The ability of *Salmonella* to enter mammalian cells is affected by bacterial growth state. Proc Natl Acad Sci U S A 87:4304–4308. https://doi.org/10.1073/pnas.87.11.4304.
37. Thanh Duy P, Thi Nguyen TN, Vu Thuy D, Chung The H, Alcock F, Boinett C, Dan Thanh HN, Thanh Tuyen H, Thwaites GE, Rabaa MA, Baker S. 2020. Commensal *Escherichia coli* are a reservoir for the transfer of XDR plasmids into epidemic fluoroquinolone-resistant *Shigella sonnei*. Nat Microbiol 5:256–264. https://doi.org/10.1038/s41564-019-0645-9.
38. Pribis JP, García-Villada L, Zhai Y, Lewin-Epstein O, Wang AZ, Liu J, Xia J, Mei Q, Fitzgerald DM, Bos J, Austin RH, Herman C, Bates D, Hadany L, Hastings PJ, Rosenberg SM. 2019. Gamblers: an antibiotic-induced evolvable cell subpopulation differentiated by reactive-oxygen-induced general stress response. Mol Cell 74:785.e7–800.e7. https://doi.org/10.1016/j.molcel.2019.02.037.
39. Bos J, Zhang Q, Vyawahare S, Rogers E, Rosenberg SM, Austin RH. 2015. Emergence of antibiotic resistance from multinucleated bacterial filaments. Proc Natl Acad Sci U S A 112:178–183. https://doi.org/10.1073/pnas.1420702111.
40. Liu P, Wu Z, Xue H, Zhao X. 2017. Antibiotics trigger initiation of SCC*mec* transfer by inducing SOS responses. Nucleic Acids Res 45:3944–3952. https://doi.org/10.1093/nar/gkx153.
41. Kelley WL. 2006. Lex marks the spot: the virulent side of SOS and a closer look at the LexA regulon. Mol Microbiol 62:1228–1238. https://doi.org/10.1111/j.1365-2958.2006.05444.x.
42. Valat C, Hirchaud E, Drapeau A, Touzain F, de Boisseson C, Haenni M, Blanchard Y, Madec J-Y. 2020. Overall changes in the transcriptome of *Escherichia coli* O26:H11 induced by a subinhibitory concentration of ciprofloxacin. J Appl Microbiol 129:1577–1588. https://doi.org/10.1111/jam.14741.
43. Ballesté-Delpierre C, Solé M, Domènech Ò, Borrell J, Vila J, Fàbrega A. 2014. Molecular study of quinolone resistance mechanisms and clonal relationship of *Salmonella enterica* clinical isolates. Int J Antimicrob Agents 43:121–125. https://doi.org/10.1016/j.ijantimicag.2013.08.017.
44. Nikaido E, Yamaguchi A, Nishino K. 2008. AcrAB multidrug efflux pump regulation in *Salmonella enterica* serovar Typhimurium by RamA in response to environmental signals. J Biol Chem 283:24245–24253. https://doi.org/10.1074/jbc.M804544200.
45. Braetz S, Schwerk P, Thompson A, Tedin K, Fulde M. 2017. The role of ATP pools in persister cell formation in (fluoro)quinolone-susceptible and -resistant strains of *Salmonella enterica* ser. Typhimurium. Vet Microbiol 210:116–123. https://doi.org/10.1016/j.vetmic.2017.09.007.
46. Rycroft JA, Gollan B, Grabe GJ, Hall A, Cheverton AM, Larrouy-Maumus G, Hare SA, Helaine S. 2018. Activity of acetyltransferase toxins involved in *Salmonella* persister formation during macrophage infection. Nat Commun 9:1993. https://doi.org/10.1038/s41467-018-04472-6.
47. Balaban NQ, Merrin J, Chait R, Kowalik L, Leibler S. 2004. Bacterial persistence as a phenotypic switch. Science 305:1622–1625. https://doi.org/10.1126/science.1099390.
48. Spoering AL, Lewis K. 2001. Biofilms and planktonic cells of *Pseudomonas aeruginosa* have similar resistance to killing by antimicrobials. J Bacteriol 183:6746–6751. https://doi.org/10.1128/JB.183.23.6746-6751.2001.
49. Keren I, Kaldalu N, Spoering A, Wang Y, Lewis K. 2004. Persister cells and tolerance to antimicrobials. FEMS Microbiol Lett 230:13–18. https://doi.org/10.1016/S0378-1097(03)00856-5.
50. Singh S, Kalia NP, Joshi P, Kumar A, Sharma PR, Kumar A, Bharate SB, Khan IA. 2017. Boeravinone B, a novel dual inhibitor of NorA bacterial efflux pump of *Staphylococcus aureus* and human P-glycoprotein, reduces the biofilm formation and intracellular invasion of bacteria. Front Microbiol 8:1868. https://doi.org/10.3389/fmicb.2017.01868.
51. González JF, Alberts H, Lee J, Doolittle L, Gunn JS. 2018. Biofilm formation protects *Salmonella* from the antibiotic ciprofloxacin *in vitro* and *in vivo* in the mouse model of chronic carriage. Sci Rep 8:222. https://doi.org/10.1038/s41598-017-18516-2.
52. Anuforom O, Wallace GR, Buckner MMC, Piddock LV. 2016. Ciprofloxacin and ceftriaxone alter cytokine responses, but not Toll-like receptors, to *Salmonella* infection *in vitro*. J Antimicrob Chemother 71:1826–1833. https://doi.org/10.1093/jac/dkw092.
53. Coldiron ME, Assao B, Page AL, Hitchings MDT, Alcoba G, Ciglenecki I, Langendorf C, Mambula C, Adehossi E, Sidikou F, Tassiou EI, De Lastours V, Grais RF. 2018. Single-dose oral ciprofloxacin prophylaxis as a response to a meningococcal meningitis epidemic in the African meningitis belt: a 3-arm, open-label, cluster-randomized trial. PLoS Med 15:e1002593. https://doi.org/10.1371/journal.pmed.1002593.
54. Keenan JD, Bailey RL, West SK, Arzika AM, Hart J, Weaver J, Kalua K, Mrango Z, Ray KJ, Cook C, Lebas E, O'Brien KS, Emerson PM, Porco TC, Lietman TM, MORDOR Study Group. 2018. Azithromycin to reduce childhood mortality in sub-Saharan Africa. N Engl J Med 378:1583–1592. https://doi.org/10.1056/NEJMoa1715474.
55. Alam T, Ahmed D, Ahmed T, Chisti MJ, Rahman MW, Asthana AK, Bansal PK, Chouhan A, Deb S, Dhingra P, Dhingra U, Dutta A, Jaiswal VK, Kumar J, Pandey A, Sazawal S, Sharma AK, McGrath C, Nyabinda C, Okello M, Pavlinac PB, Singa B, Walson JL, Bar-Zeev N, Dube Q, Freyne B, Ndamala C, Ndeketa L, Badji H, Booth JP, Coulibaly F, Haidara F, Kotloff K, Malle D, Mehta A, Sow S, Tapia M, Tennant S, Hotwani A, Kabir F, Qamar F, Qureshi S, Shakoor S, Thobani R, Yousufzai MT, Bakari M, Duggan C, Kibwana U, Kisenge R, Manji K, et al. 2020. A double-blind placebo-controlled trial of azithromycin to reduce mortality and improve growth in high-risk young children with non-bloody diarrhoea in low resource settings: the Antibiotics for Children with Diarrhoea (ABCD) trial protocol. Trials 21:71. https://doi.org/10.1186/s13063-019-3829-y.
56. Doan T, Hinterwirth A, Worden L, Arzika AM, Maliki R, Abdou A, Kane S, Zhong L, Cummings SL, Sakar S, Chen C, Cook C, Lebas E, Chow ED, Nachamkin I, Porco TC, Keenan JD, Lietman TM. 2019. Gut microbiome alteration in MORDOR I: a community-randomized trial of mass azithromycin distribution. Nat Med 25:1370–1376. https://doi.org/10.1038/s41591-019-0533-0.
57. Hoiseth SK, Stocker BA. 1981. Aromatic-dependent *Salmonella* Typhimurium are non-virulent and effective as live vaccines. Nature 291:238–239. https://doi.org/10.1038/291238a0.
58. R Core Development Team. 2017. R: a language and environment for statistical computing. R Foundation for Statistical Computing, Vienna, Austria.
59. Wickham H. 2016. ggplot2: elegant graphics for data analysis (Use R!). Springer-Verlag, New York, NY.
60. Love MI, Huber W, Anders S. 2014. Moderated estimation of fold change and dispersion for RNA-seq data with DESeq2. Genome Biol 15:550. https://doi.org/10.1186/s13059-014-0550-8.
61. Alexa A, Rahnenfuhrer J. 2020. topGO: enrichment analysis for gene ontology. 2.42.0. https://bioconductor.org/packages/release/bioc/html/topGO.html.

62. Mäklin T, Kallonen T, David S, Boinett CJ, Pascoe B, Méric G, Aanensen DM, Feil EJ, Baker S, Parkhill J, Sheppard SK, Corander J, Honkela A. 2020. High-resolution sweep metagenomics using fast probabilistic inference. Wellcome Open Res 5:14. https://doi.org/10.12688/wellcomeopenres.15639.1.
63. Van Puyvelde S, Pickard D, Vandelannoote K, Heinz E, Barbé B, de Block T, Clare S, Coomber EL, Harcourt K, Sridhar S, Lees EA, Wheeler NE, Klemm EJ, Kuijpers L, Mbuyi Kalonji L, Phoba MF, Falay D, Ngbonda D, Lunguya O, Jacobs J, Dougan G, Deborggraeve S. 2019. An African *Salmonella* Typhimurium ST313 sublineage with extensive drug-resistance and signatures of host adaptation. Nat Commun 10:1–12. https://doi.org/10.1038/s41467-019-11844-z.
64. Hale C, Yeung A, Goulding D, Pickard D, Alasoo K, Powrie F, Dougan G, Mukhopadhyay S. 2015. Induced pluripotent stem cell derived macrophages as a cellular system to study *Salmonella* and other pathogens. PLoS One 10:e0124307. https://doi.org/10.1371/journal.pone.0124307.
65. Sridhar S, Forrest S, Warne B, Maes M, Baker S, Dougan G, Bartholdson Scott J. 2021. High-content imaging to phenotype antimicrobial effects on individual bacteria at scale. mSystems 6:e00028–21. https://doi.org/10.1128/mSystems.00028-21.